CERN – EUROPEAN ORGANIZATION FOR NUCLEAR RESEARCH

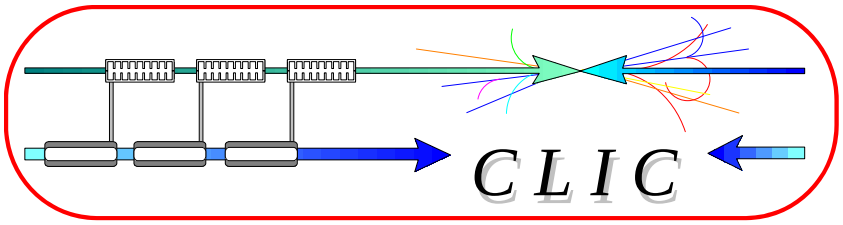

CLIC-Note-808

STUDY OF AN HYBRID POSITRON SOURCE USING CHANNELING FOR CLIC

Olivier Dadoun[1], Iryna Chaikovska[1], Robert Chehab[2], Freddy Poirier[1]
Louis Rinolfi[3], Vladimir Strakhovenko[4], Alessandro Variola[1], Alessandro Vivoli[3]

[1]- LAL, IN2P3-CNRS and Université de Paris Sud, 91898 Orsay Cedex, France
[2]- IPN- Lyon, IN2P3-CNRS and Université Claude Bernard, 69622 Villeurbanne, France
[3]- CERN, CH-1211 Genève 23, Switzerland
[4]- BINP, Av. Lavrentyeva, 11, 630090 Novosibirsk, Russia

Abstract

The CLIC study considers the hybrid source using channeling as the baseline for positron production. The hybrid source uses a few GeV electron beam impinging on a crystal tungsten radiator. With the tungsten crystal oriented on its < 111 > axis it results an intense, relatively low energy photon beam due mainly to channeling radiation. Those photons are then impinging on an amorphous tungsten target producing positrons by e+e− pair creation. In this note the optimization of the positron yield and the peak energy deposition density in the amorphous target are studied according to the distance between the crystal and the amorphous targets, the primary electron energy and the amorphous target thickness.

Geneva, Switzerland
September 2009

1 Introduction

Due to the heating problem and large emittance values of the positrons emerging from the target, the conventional positron source would not be employed either for CLIC [1] nor ILC [2] colliders. A promising method, considered as the baseline for the CLIC positron production, is based on a combined crystal and amorphous tungsten target [3]. The large number of photons produced in axial channeling in a crystal from GeV electron beam leads to a subsequent large number of pairs in an amorphous tungsten target. A capture section based on a slowly (adiabatically) decreasing magnetic field system is used to collect the positrons after the target before being accelerated [4].

To limit the energy deposition in the amorphous target, the charged particles will be swept off after the crystal. The space between the crystal and the amorphous target is then used to install a dipole magnet to bend the charged particles.
As the distance increases, the photon beam spot size at the entrance of the amorphous target will increase. It results in decreasing positron capture efficiency and diminution of energy per unit volume in the amorphous target. The density of impinging photons on the amorphous target decreases relaxing the Peak Energy Deposition Density (PEDD) constraints [5], which is limited for an amorphous tungsten target to 35 J/g, value based on the result of the SLC damaged target analysis [6]. Therefore this distance must be optimized between a minimum value for the PEDD and a maximum value for the positron yield.

2 Simulation

Different incident electron beam energies impinging on the crystal are considered for this study namely between 3 and 10 GeV. The primary electron beam parameters requested for the 3 TeV CLIC charge are the following [1] :

- Number of electrons per bunch : 7.5×10^9
- Number of bunches per train : 312
- Number of electrons per train : 2.34×10^{12}
- Repetition frequency : 50 Hz
- Spot size (radius) : 2.5 mm, at the crystal target

For the CLIC 0.5 TeV configuration, the electron and positron charge per bunch is doubled. Another study will cover the requests for the 0.5 TeV configuration.

As the charged particles are bent after the crytal and are not impinging on the amorphous converter we will only consider the photons distribution. The generation of the photons from the crystal tungsten target was obtained using the Strakhovenko's simulation code [7]. Details about the photon beam characteristics are given below.

Geant4 toolkit [8] was used to simulate the pair production, the beam power deposition inside the amorphous target and the first element of the capture section.

2.1 Crystal target

The crystal axis $< 111 >$ is aligned on the direction of the few GeV impinging electron beam. According to the incident electron beam energy, different radiator thicknesses have been chosen. They correspond to some optimum values [4, 7]. Table 1 shows these values for different primary electron beam energies.

E_{e^-}(GeV)	P_{e^-}(kW)	t(cm)	N_γ/e^-	$\overline{E}_\gamma$(MeV)	P_γ(kW)
10	190	0.10	22.5	304	130
5	90	0.14	20.0	160	58
4	72	0.15	18.5	136	45
3	54	0.16	15.5	115	32

Table 1: Incident electron energy E_{e^-} and corresponding beam power P_{e^-}, crystal thickness "t", number of photons N_γ per incident electron, photon mean energy $\overline{E}_\gamma$ and corresponding photon power P_γ.

The power deposited in the crystal has been investigated theoretically at incident energies of $2 - 10$ GeV [5] and experimentally at 4 GeV [9] and could be neglected for those thicknesses. They are below 1% of the incident power electron beam energy. Due to channeling radiation an intense photon flux emerges at the exit of the radiator. The energy distribution (Figure 1) is peaked in the low energy range compared to the incident electron beam energy. For 10 GeV incident electron beam the mean photon energy is about 300 MeV (60% of the photons below 100 MeV) being roughly 3 times less for 3 GeV (75% of the photons below 100 MeV) (Table 1).

2.2 Amorphous target and AMD simulation

The amorphous target and the first element of the magnetic capture section were simulated using Geant4 simulation. Due to its high heat capacity, the amorphous target is taken in pure tungsten material ($\rho = 19.3$ g/cm^3 and radiation length of $X_0 = 0.35$ cm). It was simulated as a parallelepiped of 2.5 cm transverse size and parametrized thickness between 0.6 cm and 1.2 cm. This volume is sliced to define elementary volumes of $0.05 \times 0.05 \times 0.1$ cm^3 to store particles spatial coordinates and energy deposition. In the amorphous tungsten an energy cut-off corresponding to 14 keV for charged particle and 10 times less for photons was taken [a].

The Adiabatic Matching Device (AMD) was chosen as the first element of the capture section. It was simulated as a cylinder of 50 cm long and 2 cm radius with

[a] This correspond for Geant4 to a range cut-off of 1 μm.

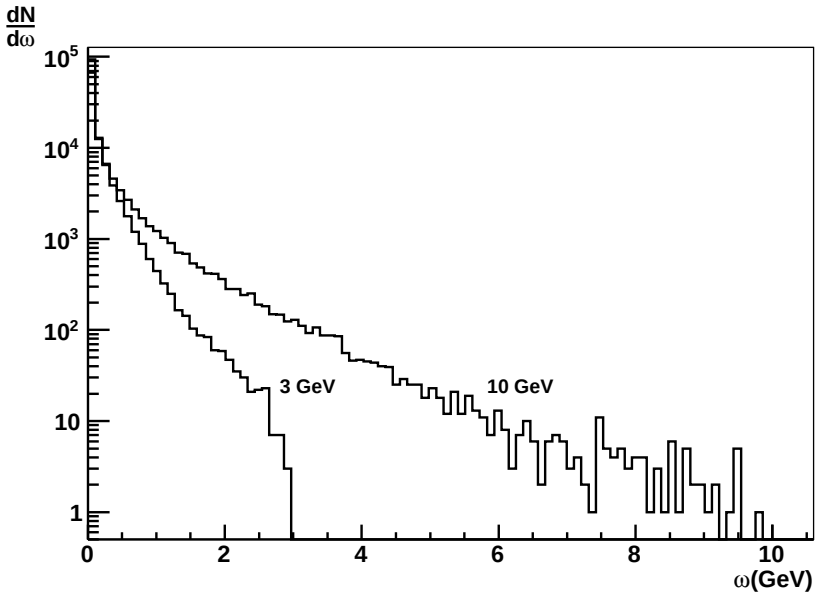

Figure 1: Photon energy distribution at the exit of the tungsten crystal target for 3 and 10 GeV incident electron beam.

a magnetic field law given by:

$$\mathrm{B} = \frac{\mathrm{B}_0}{1+\alpha \mathrm{z}}, \text{with } \mathrm{B}_0 = 6 \text{ T and } \alpha = 22\,\mathrm{m}^{-1}.$$

After the AMD the positron emittance is described by an ellipse with large radial dimension and small transverse momentum as shown in Figure 2. The associated positron energy is presented in Figure 3. Basically the AMD transform the positron phase space after the target into a larger dimensions and smaller momentum which will be easier to transport.

3 Results

3.1 Positron yield and PEDD

The positron yield is defined as the ratio of the number of positron after the AMD and the number of electrons which impinge on the crystal radiator. On Table 2 we present -for a thickness of 1.2 cm and a distance between the radiator and the target of 2 m- the yield, the total energy deposited in the target and the PEDD for different incident electron beam energies. At 10 GeV the yield is 4.14, about 4 times higher than at 3 GeV and 2 times than at 5 GeV. The total power deposited in the amorphous target as a function of the target thickness is presented on Figure 4 for different electron beam energies. For the amorphous target of 1.2 cm thickness, a distance radiator-converter of 2 m 22.45 kW are deposited for10 GeV electron beam energy, and 13.45 kW for 5 GeV. The PEDD constraint imposes not to exceed the

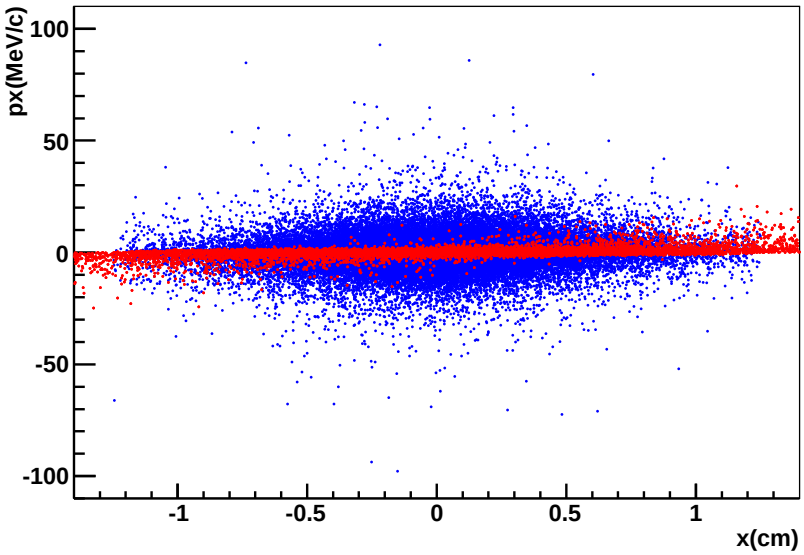

Figure 2: Positron emittances before and after AMD (a zoom on px values was applied). Target thickness is 1.0 cm, distance radiator-target is 2 m and incident electron beam energy is 5 GeV.

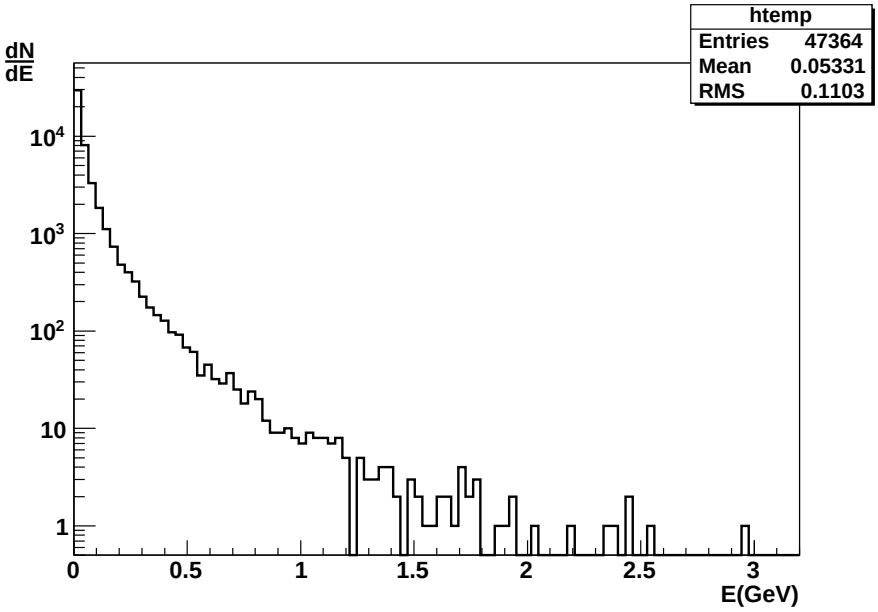

Figure 3: Positron energy distribution associated to the Figure 2. Mean positron energy is 53 MeV. About 90% of the positrons are below 200 MeV.

35 J/g, so the 10 GeV electron beam energy can not be used for that thickness but with thinner ones.
The shape of the shower distribution around the PEDD is represented on Figure 5

and the total energy deposited in the amorphous converter on Figure 6. Let us note that the maximum deposition occured at the end of the target.

E_{e^-}(GeV)	Yield	P(kW)	Pedd(J/g)
3	1.04	7.9	10.30
4	1.50	10.8	16.90
5	1.95	13.4	24.27
10	4.14	22.4	59.81

Table 2: Incident electron beam energy E_{e^-}, positron yield, power deposited and PEDD for distance between the crystal and the amorphous of 2 m and a target thickness of 1.2 cm.

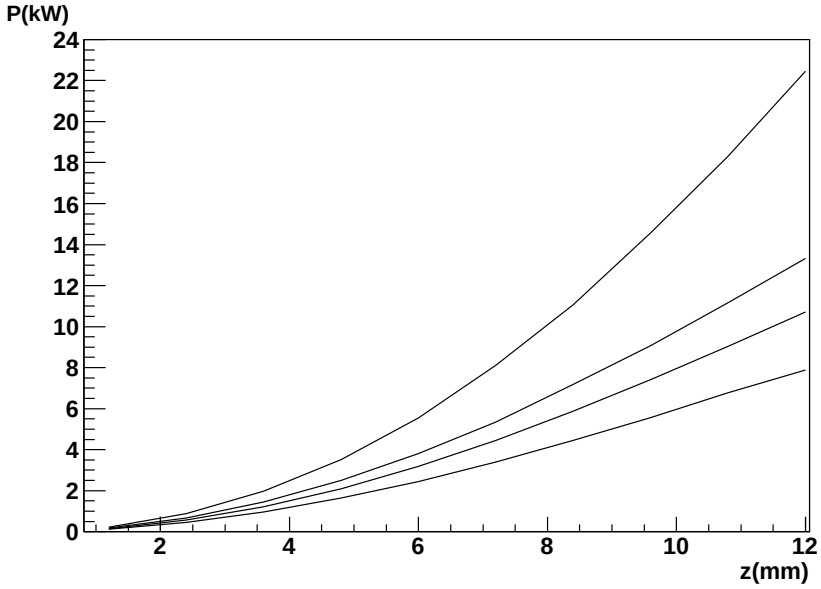

Figure 4: Power deposited with respect to the target thickness z. From up to bottom 10, 5, 4 and 3 GeV electron beam energies.

3.2 Radiator-target distance studies

To limit the power energy deposition in the target the charged particles are swept off. The space between radiator and target is used to bend charged particles; increasing this distance will decrease the PEDD (Figure 7) but also slightly the yield (Figure 8). A compromise must be found.

Figure 8 shows that the positron yield is not so affected by the variation of the distance crystal-amorphous, a diminution of a few percent is observed from 1.5 to 3 m. This is due to the large geometrical acceptance of the AMD (about 6 mm

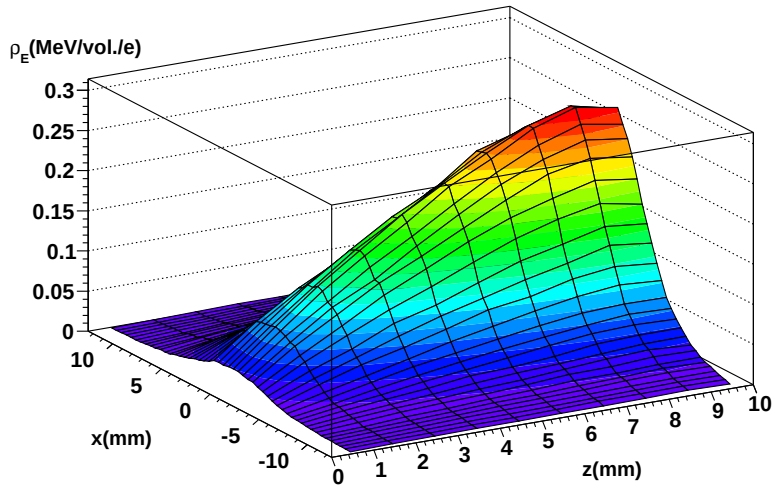

Figure 5: Energy deposition density for elementary volume of 2.5×10^{-4} cm^3 per electron from photons initiated by electrons of 5 GeV beam energy. The distance crystal-amorphous is 2 m.

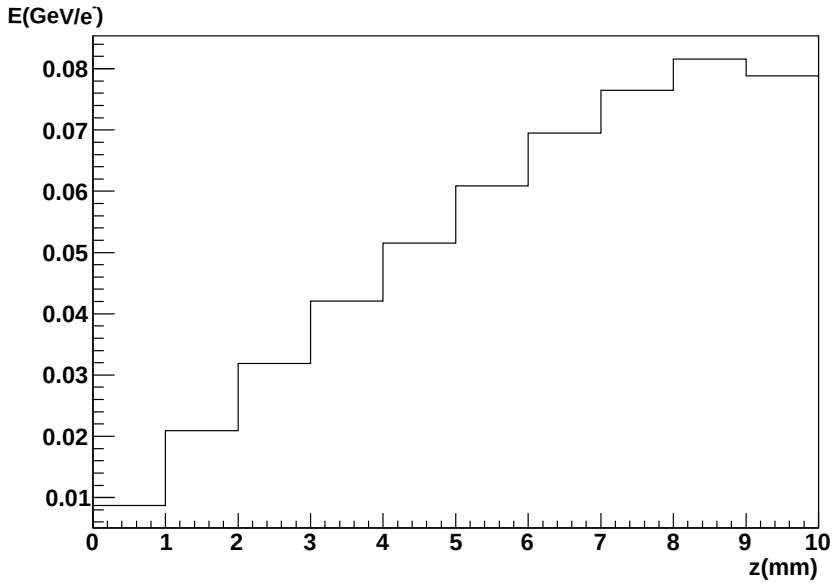

Figure 6: Total energy deposited in the amorphous target along the thickness (5GeV beam energy).

radius). At contrary the PEDD is more sensible to the distance variation. On Figure 7 we can see a diminution of the order of a few tens percents between 1.5 and 3 m. To perform a parametric evaluation of the PEDD and the positron yield a systematic study have been done for different incident electron beam energies,

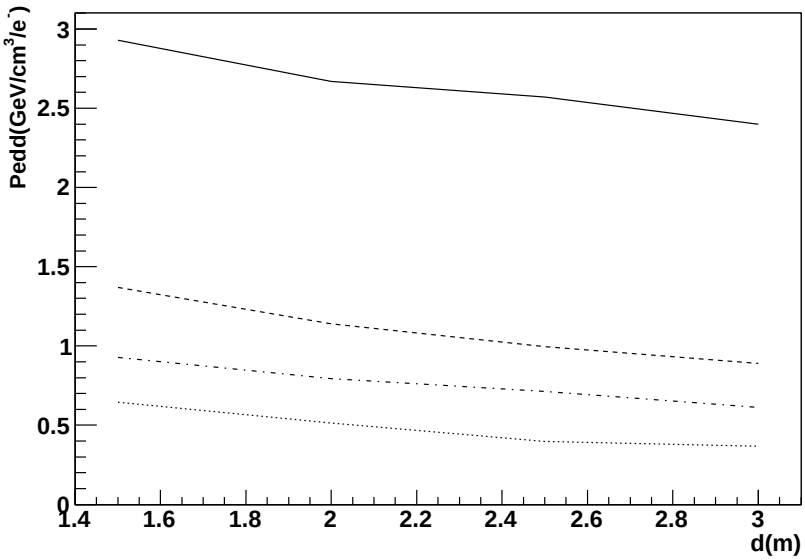

Figure 7: The PEDD versus the distance between radiator and converter(for 1 cm amorphous target tungsten). From up to bottom 10, 5, 4 and 3 GeV electron beam energies.

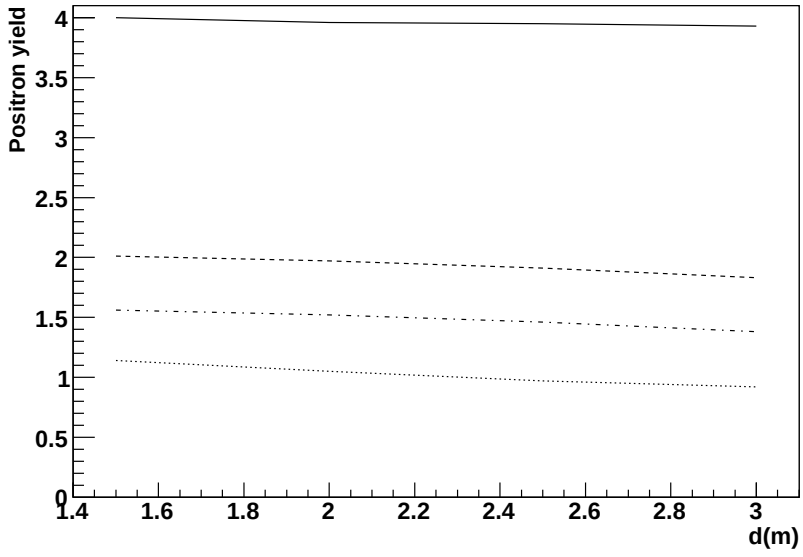

Figure 8: Positron yield versus the distance between the radiator and converter (for 1 cm amorphous target tungsten). From up to bottom 10, 5, 4 and 3 GeV electron beam energies.

different distances between radiator-converter and different radiator and converter thicknesses. This is summarized in Tables 3, 4, 5 and 6.

e(cm)	d(m)	Yield	P(kW)	Pedd (GeV/cm^3/e$^-$)	Pedd(J/g/train)
0.6	1.5	1.05	2.60	0.47	9.13
0.6	2.0	0.98	2.45	0.37	7.20
0.6	2.5	0.92	2.30	0.33	6.41
0.6	3.0	0.87	2.20	0.28	5.44
0.8	1.5	1.10	4.30	0.57	11.07
0.8	2.0	1.04	4.10	0.45	8.74
0.8	2.5	0.97	3.90	0.37	7.20
0.8	3.0	0.90	3.60	0.37	7.20
1.0	1.5	1.14	6.30	0.65	12.62
1.0	2.0	1.05	5.95	0.52	10.10
1.0	2.5	0.97	5.60	0.40	7.77
1.0	3.0	0.92	5.25	0.37	7.20
1.2	1.5	1.12	8.40	0.65	12.62
1.2	2.0	1.04	7.90	0.53	10.30
1.2	2.5	0.96	7.45	0.45	8.74
1.2	3.0	0.90	7.05	0.37	7.20

Table 3: 3 GeV incident electron beam energy.

e(cm)	d(m)	Yield	P(kW)	Pedd (GeV/cm^3/e$^-$)	Pedd(J/g/train)
0.6	1.5	1.44	3.30	0.72	14.00
0.6	2.0	1.38	3.20	0.65	12.62
0.6	2.5	1.29	3.05	0.50	9.71
0.6	3.0	1.27	2.95	0.48	9.32
0.8	1.5	1.54	5.55	0.80	15.54
0.8	2.0	1.49	5.40	0.74	14.37
0.8	2.5	1.41	5.20	0.60	11.65
0.8	3.0	1.36	5.00	0.54	10.49
1.0	1.5	1.56	8.20	0.93	18.06
1.0	2.0	1.52	8.00	0.80	15.54
1.0	2.5	1.46	7.70	0.71	13.80
1.0	3.0	1.38	7.30	0.61	11.85
1.2	1.5	1.56	11.15	1.02	19.81
1.2	2.0	1.50	10.80	0.87	16.90
1.2	2.5	1.45	10.35	0.79	15.34
1.2	3.0	1.39	10.00	0.64	12.43

Table 4: 4 GeV incident electron beam energy.

e(cm)	d(m)	Yield	P(kW)	Pedd (GeV/cm^3/e$^-$)	Pedd(J/g/train)
0.6	1.5	1.83	3.90	0.95	18.45
0.6	2.0	1.76	3.85	0.83	16.12
0.6	2.5	1.70	3.70	0.71	13.80
0.6	3.0	1.66	3.65	0.64	12.43
0.8	1.5	2.00	6.70	1.17	22.72
0.8	2.0	1.91	6.55	1.00	19.42
0.8	2.5	1.87	6.40	0.87	16.90
0.8	3.0	1.81	6.20	0.78	15.15
1.0	1.5	2.01	10.05	1.37	26.60
1.0	2.0	1.97	9.80	1.14	22.14
1.0	2.5	1.91	9.60	1.00	19.42
1.0	3.0	1.83	9.25	0.89	17.29
1.2	1.5	2.04	13.70	1.41	27.38
1.2	2.0	1.95	13.45	1.25	24.27
1.2	2.5	1.92	13.05	1.05	20.40
1.2	3.0	1.86	12.65	0.96	18.65

Table 5: 5 GeV incident electron beam energy.

e(cm)	d(m)	Yield	P(kW)	Pedd (GeV/cm^3/e$^-$)	Pedd(J/g/train)
0.6	1.5	3.23	5.60	1.83	35.54
0.6	2.0	3.30	5.60	1.78	34.57
0.6	2.5	3.26	5.55	1.58	30.69
0.6	3.0	3.24	5.50	1.50	29.13
0.8	1.5	3.67	10.20	2.54	49.33
0.8	2.0	3.66	10.05	2.25	43.70
0.8	2.5	3.62	10.00	2.14	41.56
0.8	3.0	3.63	9.95	1.98	38.45
1.0	1.5	4.00	15.80	2.93	56.90
1.0	2.0	3.96	15.75	2.67	51.85
1.0	2.5	3.95	15.65	2.57	49.91
1.0	3.0	3.93	15.50	2.40	46.61
1.2	1.5	4.15	22.50	3.17	61.56
1.2	2.0	4.14	22.45	3.08	59.81
1.2	2.5	4.16	22.40	2.98	57.87
1.2	3.0	4.05	22.25	2.87	55.74

Table 6: 10 GeV incident electron beam energy.

From those tables we can conclude that PEDD constraint is almost always satisfied for 3, 4 and 5 GeV. For 10 GeV it is only possible for thickness below 0.6 cm.

4 Conclusion

Aiming to obtain a high enough positron yield and a PEDD below the limit value of 35J/g for a tungsten target, different parameters (incident energy, radiator-converter distance, converter thickness) could be chosen. Concerning the CLIC requirements and looking at the tables for the four energies considered:
- for the higher energy of 10 GeV, the choice is restricted to converter thickness below 0.6 cm.
- for 3, 4 and 5 GeV, almost all the combination of converter thickness, radiator-converter distances are acceptable with positron yield greater than 1. However, as the accepted yield are taken at the exit of the matching device, a safety factor must be taken into account to ensure acceptable yield ($1\ e^+/e^-$) at the entrance of the predamping ring. In that case a good compromise between yield and PEDD is:

- an incident electron energy of 5 GeV
- a distance radiator-converter between 2 and 3 meters
- a converter thickness between 6 and 8 mm.

References

[1] L. Rinolfi, "CLIC Main Beam Injector Complex-Review and status" CLIC workshop 2008, CERN, CH.

[2] J. Clarke, "Positron source update", ILC08, Chicago, USA.

[3] R. Chehab et al. Study of a positron source generated by photons from ultrarelativistics channeled particles - 1989 PAC, Chicago, March 1989.

[4] X. Artru et al., NIMB 266 (2008) 3868.

[5] X. Artru et al., Phys. Rev. ST-AB 6 (2003) 091003.

[6] S. Maloy et al., LANL Report No. LA-UR-01-1913.

[7] V. Strakhovenko private communication.

[8] S. Agostinelli et al. "Geant4 - a simulation toolkit", NIM - A 206 (2003), 250-303.

[9] T. Suwada et al., Phys. Rev. ST-AB 10, 073501 (2007).